Letter

# Nonlocal current-driven heat flow in ideal plasmas

Nicholas Mitchell [1], David Chapman [2], and Grigory Kagan [1]
[1] *The Blackett Laboratory, Imperial College, London SW7 2AZ, United Kingdom*
[2] *First Light Fusion Limited, Unit 9/10 Oxford Pioneer Park, Mead Road, Yarnton, Kidlington OX5 1QU, United Kingdom*

(Received 23 July 2025; accepted 7 November 2025; published 24 November 2025)

Electron heat flux is an important and often dominant mechanism of energy transport in a variety of collisional plasmas in a confined fusion or astrophysical context. While nonlocal conductive heat transport, driven by strong temperature gradients, has been investigated extensively in previous literature, nonlocal regimes of the current-driven heat flow and friction have not received the same attention. In this Letter, a first-principles reduced kinetic method is applied to study nonlocal effects on current-driven transport. In addition to nonlocality due to sharp gradients, sufficiently large currents are found to significantly enhance current-driven heat flux due to a novel nonlocal mechanism, with this enhancement being increasingly prevalent for higher effective ionizations $Z^*$. Introducing the dimensionless number $N_u \equiv |\boldsymbol{u}_e - \boldsymbol{u}_i|/v_{\mathrm{th},e}$, these enhancements occur for even relatively weak flows $N_u \gtrsim 1/100$, analogously to standard nonlocal effects becoming significant for Knudsen numbers $N_K \gtrsim 1/100$.

DOI: 10.1103/jn8x-nfv2

It has long been established that in a wide range of practically important scenarios the electron heat conduction becomes nonlocal even when the plasma appears close to local thermal equilibrium (LTE) [1–8]. Standard Chapman-Enskog-type calculations [9–13] yield a local analytic expression for the electron conductive heat flux $\boldsymbol{q}_e^T \propto -\nabla T_e$ that breaks down even for seemingly small Knudsen numbers [14]. This Knudsen number is conventionally defined as $N_K = \lambda_{\mathrm{th}}/L$, where $\lambda_{\mathrm{th}}$ is the thermal mean free path (MFP) and $L \sim |\nabla T_e/T_e|^{-1}$ is the gradient length scale of the electron temperature. The ultimate reason for the conductive heat flux becoming nonlocal even for seemingly smooth temperature profiles is that heat is transported predominantly by electrons with velocities $v \lesssim 4v_{\mathrm{th},e}$, where $v_{\mathrm{th},e} = \sqrt{2k_B T_e/m_e}$ is the electron thermal velocity. In plasmas, a charged particle's MFP scales as the fourth power of the particle velocity $\lambda_{\mathrm{th}} \propto v^4$, so the MFPs of electrons relevant to heat transport can be comparable to $L$ even if $N_K \ll 1$, leading to nonlocal deviations of $\boldsymbol{q}_e^T$.

Owing to the large practical importance of heat transport in plasmas, extensive literature focuses on the conductive electron heat flux. The physics behind its nonlocality is well understood, as outlined above; first-principles studies have been carried out [14–17] and computationally efficient nonlocal closures have been developed [18–24]. What has largely been overlooked, however, is the nonlocal physics of the current-driven heat flow, in the plasma context known as $\boldsymbol{q}_e^u \propto \Delta\boldsymbol{u} \equiv \boldsymbol{u}_e - \boldsymbol{u}_i = -\boldsymbol{j}/en_e$ of Braginskii's seminal monograph [11], which describes the Peltier and Ettingshausen effects. Although considered in a few works, nonlocal modifications to $\boldsymbol{q}_e^u$ have been attributed to the same spatial scales based on the Knudsen number [25,26]. Since these works relied on simplified rather than first-principles approaches with this assumption essentially built in, a novel driver of the nonlocal behavior, the electron flow itself, has been missed.

In this Letter, we demonstrate that the dimensionless number $N_u \equiv |\Delta\boldsymbol{u}|/v_{\mathrm{th},e}$ plays a role to $\boldsymbol{q}_e^u$ analogous to that $N_K$ plays for $\boldsymbol{q}_e^T$. Although one might expect that the standard local calculation is valid with $N_u \ll 1$, a much more restrictive condition is found to be required. Both an intuitive explanation of the underlying transport physics and first-principles kinetic calculations are presented. A similar but smaller effect is also found on the electron-ion friction $\boldsymbol{R}_e^u$. Deviations from standard results due to this effect are increasingly prevalent at higher effective ionizations $Z^* \equiv \langle Z^2\rangle/\langle Z\rangle$ since the relative importance of electron-ion collisions over electron-electron collisions is increased.

Local heat conduction in a collisional magnetized plasma is widely understood, originating from the random motion of electrons that diffuses heat due to a temperature gradient. Analysis of small-angle binary Coulomb collisions shows that the collision frequency of a test electron against an ion background is inversely proportional to the cube of its speed in the frame comoving with the ion population, i.e., $\nu_{ei} \propto 1/|\boldsymbol{v} - \boldsymbol{u}_i|^3$. This fact has the consequence that relative flows, or currents, also drive heat flux as electrons moving in the same direction as the relative drift ($\boldsymbol{w} \cdot \Delta\boldsymbol{u} > 0$, where $\boldsymbol{w} = \boldsymbol{v} - \boldsymbol{u}_e$ is the electron peculiar velocity) are less collisional on average against ions than electrons moving against the relative drift ($\boldsymbol{w} \cdot \Delta\boldsymbol{u} < 0$). The heat carried by these two sides of the electron population then does not cancel and there is a net heat flux in the direction of the relative flow $\boldsymbol{q}_e^u \propto \Delta\boldsymbol{u}$. Currents necessitate the inclusion of magnetic fields which cause electrons to undergo gyro-orbits around the magnetic field lines, suppressing heat transport in the direction perpendicular to the field. However, the gyro-orbits also generate particle motion

*Published by the American Physical Society under the terms of the Creative Commons Attribution 4.0 International license. Further distribution of this work must maintain attribution to the author(s) and the published article's title, journal citation, and DOI.*

in the direction perpendicular to both the magnetic field and temperature gradient or relative flow, therefore an additional "cross" component to each of the above transport fluxes is gained in this direction.

The above picture allows a qualitative explanation as to why local current-driven heat flux results [10–13] break down even for relatively weak electron flows. A nonvanishing net electron flow implies a nonzero electric field set by the bulk electron distribution. This flow being much slower than $v_{\mathrm{th},e}$ is equivalent to the electric field being much less than the Dreicer field [27]. While this ensures the bulk distribution is not in a disruptive runaway scenario, the dynamic friction experienced by suprathermal electrons is lower due to the aforementioned collision frequency scaling. Dynamic friction can then be insufficient to prevent the electric field from driving suprathermal electrons farther away from thermodynamic equilibrium than can be captured by a local transport theory. Since this mechanism accelerates electrons in the direction of the relative flow $\Delta\boldsymbol{u}$, nonlocal behavior is expected to vary for the different magnetized components of current-driven heat flow in the parallel, perpendicular, and cross directions. We now proceed to the quantitative first-principles description of these nonlocal effects.

In a sufficiently collisional simple plasma, the local results [13] for the current-driven electron heat flux and friction force are

$$\boldsymbol{q}_e^u = n_e k_{\mathrm{B}} T_e \left[ \underbrace{[\hat{\beta}_\parallel \boldsymbol{bb} + \hat{\beta}_\perp(\mathbb{I} - \boldsymbol{bb})] \cdot \Delta\boldsymbol{u}}_{\text{Peltier}} + \underbrace{\hat{\beta}_\times \boldsymbol{b} \times \Delta\boldsymbol{u}}_{\text{Ettingshausen}} \right],$$

$$\boldsymbol{R}_e^u = -\frac{n_e m_e}{\tau_{ee}} \left[ \underbrace{[\hat{\alpha}_\parallel \boldsymbol{bb} + \hat{\alpha}_\perp(\mathbb{I} - \boldsymbol{bb})] \cdot \Delta\boldsymbol{u}}_{\text{Friction}} - \underbrace{\hat{\alpha}_\times \boldsymbol{b} \times \Delta\boldsymbol{u}}_{\text{Cross-friction}} \right], \tag{1}$$

where $\tau_{ee}$ is the electron-electron collision time and $\boldsymbol{b} = \boldsymbol{B}/|\boldsymbol{B}|$ is the unit vector parallel to the magnetic field. The dimensionless coefficients $\hat{\alpha}_{\parallel,\perp,\times}$ and $\hat{\beta}_{\parallel,\perp,\times}$ are dependent on the effective ionization $Z^*$ and, for perpendicular and cross terms, the Hall parameter $\chi = \omega_{\mathrm{c},e}\tau_{ee}$ with electron cyclotron frequency $\omega_{\mathrm{c},e} = e|\boldsymbol{B}|/m_e$.

The reduced kinetic method (RKM) from previous work [28,29] has been extended to solve the Vlasov-Fokker-Planck (VFP) equation for the deviation of the electron distribution function from Maxwellian $\delta f_e = f_e - f_e^M$ in one-spatial three-velocity (1D3V) coordinates $(z, \boldsymbol{w})$ given input fluid profiles. The RKM evaluates nonlocal transport from the input profiles, in contrast with a full VFP simulation which relies on evaluating transport quantities from relaxing profiles, which may have changed significantly from the input profiles before the quasistationary transport fluxes are established. Here, this method is applied to electrons, where the VFP equation for $\delta f_e$ in the frame moving with the local electron flow $\boldsymbol{u}_e$ is

$$f_e^M \left[ \left( \boldsymbol{R}_e/p_e + \left( \frac{w^2}{v_{\mathrm{th},e}^2} - \frac{5}{2} \right) \nabla \ln T_e \right) \cdot \boldsymbol{w} + \frac{2}{v_{\mathrm{th},e}^2} \nabla\boldsymbol{u}_e : \left( \boldsymbol{ww} - \frac{1}{3} w^2 \mathbb{I} \right) \right] - C_{ei}\{f_e^M\}$$

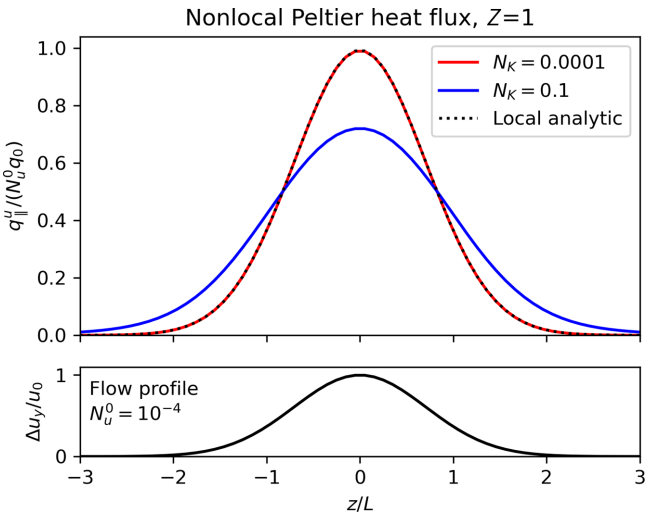



FIG. 1. Current-driven Peltier heat flux in a simple unmagnetized isothermal isochoric hydrogen ($Z^* = 1$) plasma with a peak flow $N_u^0 = |u_0|/v_{\mathrm{th},e} = 10^{-4}$. The heat flux is appropriately normalized against $N_u$ and the free-streaming heat flux $q_0 = n_e k_{\mathrm{B}} T_e v_{\mathrm{th},e}/\sqrt{2}$. For small Knudsen number $N_K = 10^{-4}$, the local analytic result for the Peltier heat flux $\boldsymbol{q}_e^u = \hat{\beta}_\parallel n_e k_{\mathrm{B}} T_e \Delta\boldsymbol{u}$, where $\hat{\beta}_\parallel(Z^* = 1) \approx 0.71$, is reproduced. For Knudsen number $N_K = 0.1$, the Peltier heat flux is noticeably nonlocal, with the peak heat flux reduced and "preheat," where the heat flux away from the peak is enhanced.

$$= C_{ee}\{\delta f_e\} + C_{ei}\{\delta f_e\} + \frac{e}{m_e}(\boldsymbol{w} \times \boldsymbol{B}) \cdot \nabla_{\boldsymbol{w}} \delta f_e - \left[ \boldsymbol{w} \cdot \nabla - \left( \boldsymbol{w} \cdot \nabla\boldsymbol{u}_e + \frac{\boldsymbol{R}_e - \nabla p_e}{\rho_e} \right) \cdot \nabla_{\boldsymbol{w}} \right] \delta f_e. \tag{2}$$

The distribution function $\delta f_e$ is expanded over spherical harmonics in velocity space, leaving a set of partial differential equations which are solved numerically. The solution for $\delta f_e$ should not perturb the flow which is considered as an input quantity, therefore should satisfy $\int d^3\boldsymbol{w}\, \boldsymbol{w} \delta f_e = \boldsymbol{0}$, which is enforced as a constraint in the solver. The heat flux is obtained as $\boldsymbol{q}_e = \int d^3\boldsymbol{w} \frac{1}{2} m_e w^2 \boldsymbol{w} \delta f_e$. To obtain the solution with a self-consistent momentum exchange $\boldsymbol{R}_e$, the RKM solver is run iteratively, passing in the integrated $\boldsymbol{R}_e = \int d^3\boldsymbol{v}\, m_e \boldsymbol{v} C_{ei}\{f_e\}$ from the previous iteration as the input $\boldsymbol{R}_e$ appearing in Eq. (2) until they match. This usually takes only one or two iterations.

To investigate the nonlocality of current-driven transport, we consider an isothermal isochoric simple plasma with a flow in the $y$ direction of the form

$$\Delta\boldsymbol{u} = u_0 \exp[-(z/L)^2]\hat{\boldsymbol{y}}, \tag{3}$$

with a uniform magnetic field in the $-x$ direction $\boldsymbol{B} = -B_0\hat{\boldsymbol{x}}$ and no ion flow $\boldsymbol{u}_i = \boldsymbol{0}$. The peak electron flow with $N_u^0 \equiv |u_0|/v_{\mathrm{th},e}$ describes the maximum speed of the flow relative to the electron thermal speed. The Knudsen number is defined as $N_K \equiv \lambda_{\mathrm{th},e}/L$, where $\lambda_{\mathrm{th},e} = \sqrt{\lambda_{\mathrm{th},ee}\lambda_{\mathrm{th},ei}}$ is the electron thermal MFP [14].

The unmagnetized Peltier heat flux $q_{e,\parallel}^u$ in a local and nonlocal case with small peak flow $N_u^0 = 10^{-4}$ is shown in Fig. 1. Similarly to the nonlocal conductive heat flux, the peak heat flux is inhibited, and the heat flux is enhanced away from the peak current. For moderate magnetic fields $\chi \sim 1$ and for

a wide variety of ionizations $Z^*$, nonlocality of the Peltier heat flux persists. Sufficiently strong magnetic fields $\chi \gg 1$ eventually suppress nonlocality, restoring the heat flux to its local limit even for high Knudsen number.

Nonlocal deviations conventionally arise from the $\boldsymbol{w} \cdot \nabla \delta f_e$ term in Eq. (2), which affects transport when

$$\frac{|\boldsymbol{w} \cdot \nabla \delta f_e|}{|C_e\{\delta f_e\}|} \sim \left(\frac{w}{v_{\mathrm{th},e}}\right)^4 N_K \tag{4}$$

is comparable to or greater than unity for particles $w/v_{\mathrm{th},e} \lesssim 4$ that contribute to transport quantities, so where $N_K \gtrsim 1/100$. However, the force term $\boldsymbol{R}_e \cdot \nabla_{\boldsymbol{w}} \delta f_e$ may also cause deviations in $\delta f_e$ and therefore transport from standard results. Ignoring spatial gradients, this term should affect transport where

$$\frac{\left|\frac{1}{\rho_e}\boldsymbol{R}_e^u \cdot \nabla_{\boldsymbol{w}} \delta f_e\right|}{|C_e\{\delta f_e\}|} \sim \left(\frac{w}{v_{\mathrm{th},e}}\right)^3 N_u \tag{5}$$

is comparable to or greater than unity for relevant particle velocities, so where $N_u \gtrsim 1/100$. If all spatial gradient terms are neglected but the force term is included, solutions to $\delta f_e$ cannot satisfy $\delta f_e(w \to \infty) = 0$ since there always exists a sufficiently large velocity in the tail where electrons become prone to runaway, leading to a divergent solution. However, these runaway electrons in the $w_y$ direction can be depleted by spatial advection in the $z$ direction acting as a sink at large $w$. For sufficiently large length scales in the $z$ direction, this spatial advection can operate at sufficiently high $w$ beyond the velocity space that contributes to the integrand of the heat flux $w \lesssim 4v_{\mathrm{th},e}$ such that the heat flux is not affected by spatial advection, so remains local. Sufficiently large flows can then cause deviations from traditional local transport calculations due to the force term which rely on spatial advection to be convergent, but yield transport fluxes which are dependent on $z$ only through the local flow $\Delta \boldsymbol{u}$, i.e., $\boldsymbol{q}_e^u = \boldsymbol{q}_e^u(\Delta \boldsymbol{u}(\boldsymbol{x}))$ and similarly for $\boldsymbol{R}_e^u$, therefore are "quasilocal." Analogously to the Knudsen number $N_K$ characterizing the impact of nonlocal effects due to spatial advection from the $\boldsymbol{w} \cdot \nabla$ operator, the number $N_u$ characterizes the impact of quasilocal effects due to velocity-space advection from the $\boldsymbol{R}_e^u \cdot \nabla_{\boldsymbol{w}}$ operator. For higher $Z^*$, the friction force against ions increases relative to the energy scattering components of the collision operator, which come only from electron-electron collisions since $m_i \gg m_e$. The quasilocal effect should then be more prevalent in higher $Z^*$ plasmas.

Figure 2 demonstrates the impact of fast flows on the Ettingshausen heat flux for $Z^* = 20$. Typical qualitative nonlocal behavior is exhibited for low $N_u^0$. For larger $N_u^0$, the heat flux is noticably modified due to the quasilocal effect arising from the $\boldsymbol{R}_e^u \cdot \nabla_{\boldsymbol{w}} \delta f_e$ term in the kinetic equation. For a small Knudsen number $N_K = 10^{-4}$, the heat flux is enhanced at large $N_u$, but remains spatially local. For a larger Knudsen number, conventional nonlocal effects make the heat flux profile nonlocal in space, reducing and shifting the peak heat flux to $z < 0$, and developing significant preheats in regions of small $N_u$. The friction and cross-friction are not shown here since they have very small $\lesssim$5% deviations from local results.

Figure 3 emphasizes the quasilocal effect by plotting the ratio against the local result as a function of $N_u = |\Delta \boldsymbol{u}/v_{\mathrm{th},e}|$. The red line for a small Knudsen number $N_K = 10^{-4}$ is

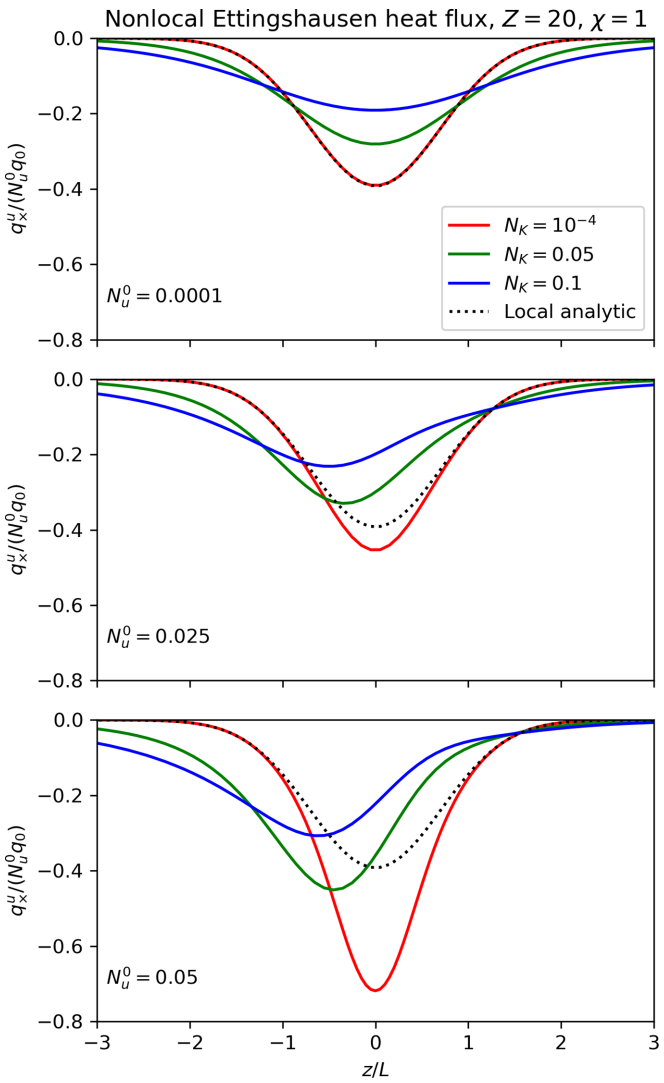



FIG. 2. Ettingshausen heat flux in a magnetized isothermal isochoric simple plasma with effective ionization $Z^* = 20$ with the same shape of flow profile as in Fig. 1. A uniform magnetic field in the $-x$ direction is chosen $\boldsymbol{B} = -B_0\hat{\boldsymbol{x}}$ with a field strength that results in a Hall parameter $\chi = 1$. Different subplots correspond to different peak flows $N_u^0 = 0.0001, 0.025, 0.05$ which have a noticeable impact on the Ettingshausen heat flux.

one to one and returns to a ratio of unity as $N_u \to 0$. This indicates that the Ettingshausen heat flux is still local, i.e., $q_{e,\times}^u = q_{e,\times}^u(u(z))$, but deviates away from the standard analytic result at large $N_u \sim 0.01$–$0.05$ due to the quasilocal effect. The blue and green lines for larger Knudsen numbers form loops, indicating that the heat flux is nonlocal, i.e., $q_{e,\times}^u$ may not be expressed as a function of the local $u$. The plus and cross markers indicate two spatial positions with the same flow. For the nonlocal case, these positions have very different heat fluxes. For the $N_K = 10^{-4}$ case, the two markers overlap on the red curve, indicating that these two spatial positions still have the same heat flux. The red curve is then not specific to this exact profile, but universal for profiles with a sufficiently small Knudsen number for the given ionization and Hall parameter. Different flow profiles with $N_u^0 = 0.05$ have

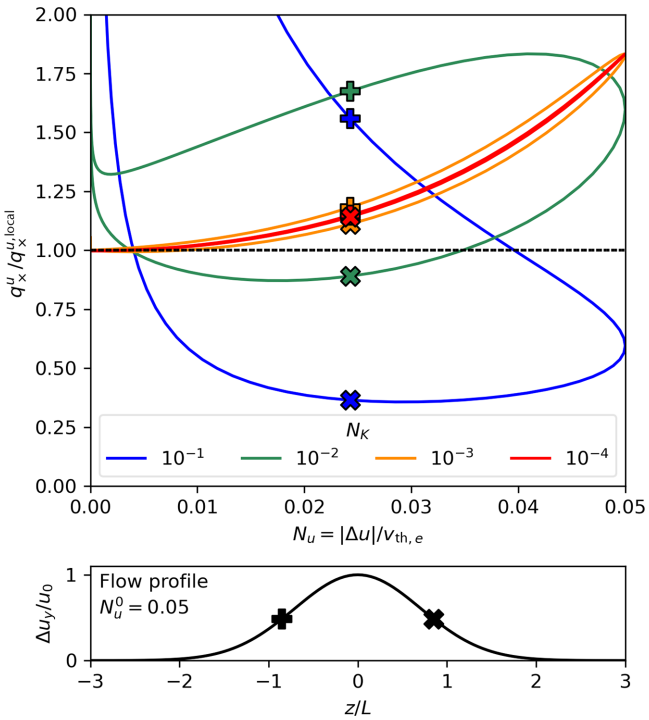



FIG. 3. Ratio of Ettingshausen heat flux to the local analytic result for peak flow $N_u^0 = 0.05$, Hall parameter $\chi = 1$, and ionization $Z^* = 20$, plotted as a function of $N_u$ rather than $z/L$ to emphasise the quasilocal effect. A wide variety of Knudsen numbers are chosen to illustrate the transition between the nonlocal and quasilocal regimes. Nonlocal heat fluxes appear as loops on these plots since they are not functions of the local flow. For a small Knudsen number, the heat flux tend towards a one-to-one line, showing that the heat flux is local. Plus and cross markers are added to indicate how different spatial positions with the same flow $N_u$ yield the same heat flow for a small Knudsen number, but different heat flow for a larger Knudsen number. A larger Hall parameter $\chi$ suppresses both nonlocal and quasilocal deviations, driving these curves closer to the black dashed line.

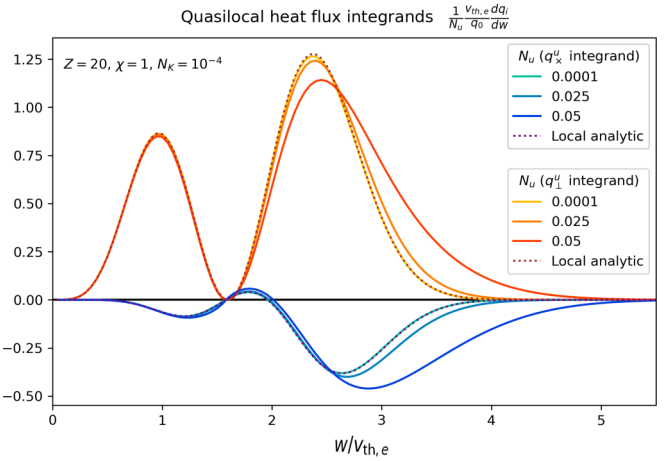



FIG. 4. Peltier and Ettingshausen heat flux integrands for various flows $N_u$ with ionization $Z^* = 20$, Hall parameter $\chi = 1$, and a very small Knudsen number $N_K \ll 1$. For small $N_u = 10^{-4}$, the heat flux integrands match up extremely well with the local analytic result. For larger $N_u \sim 0.025$–$0.05$, higher-energy electrons $w/v_{\mathrm{th},e} \gtrsim 2.5$ are accelerated, shifting the integrand to a larger velocity and enhancing the heat fluxes corresponding to the integrated area beneath the curves. The Ettingshausen integrands are more weighted to higher $w$ than the Peltier integrands, i.e., the Ettingshausen heat flow is carried preferentially by faster particles than the Peltier heat flow, explaining why the Ettingshausen heat flow is more impacted by large $N_u$.

been verified to reproduce the same red curve for a sufficiently small Knudsen number.

Figure 4 demonstrates the impact of the quasilocal effect on the integrands of the heat flux in the $y$ and $z$ directions. For high $N_u$, the integrand at low velocities $w/v_{\mathrm{th},e} \lesssim 2$ experiences only small deviations due to the $\boldsymbol{R}^u_e \cdot \boldsymbol{\nabla}_{\boldsymbol{w}} \delta f_e$ term since the bulk is highly collisional. In the less-collisional region $2 \lesssim w/v_{\mathrm{th},e} \lesssim 5$, the heat flux integrand for high $N_u$ is greatly enhanced from the local result due to electrons starting to become runaway. Electrons that do become runaway are then accelerated to larger velocities $w/v_{\mathrm{th},e} \gtrsim 5$ where they may be depleted to other regions in physical space by spatial advection, even for a very small Knudsen number. This spatial advection occurs in regions of velocity space that do not contribute significantly to the heat flux integrand, thus leaving the heat flux local. Even larger $N_u$, larger $Z^*$, or smaller $\chi$ may then result in divergent integrands, which is indicative of being so far from LTE that fluid models with quasistatic transport closures are not applicable and a full kinetic description is required, such as full VFP [1,30] or particle-in-cell simulations [31–33]. Nonlocal transport modeling is further complicated for nonideal plasmas, where nonbinary collisions and the quantum degeneracy of electrons can no longer be ignored, and computationally intense methods such as molecular dynamics simulations need to be employed [34].

In summary, current-driven electron heat flux $\boldsymbol{q}^u_e$ becomes nonlocal in the presense of relatively weak spatial gradients with the Knudsen number $N_K \equiv \lambda_{\mathrm{th},e}/L \gtrsim 1/100$, as opposed to $N_K \gtrsim 1$, similarly to the conductive heat flux $\boldsymbol{q}^T_e$. Furthermore, a novel nonlocal modification to $\boldsymbol{q}^u_e$ has been found, which is driven by a relatively weak electron flow $N_u \equiv |\boldsymbol{u}_e - \boldsymbol{u}_i|/v_{\mathrm{th},e} \gtrsim 1/100$, as opposed to $N_u \gtrsim 1$. The underlying physics has been both captured with a first-principles kinetic model and explained qualitatively and can significantly modify and enhance Ettingshausen heat flow. Such effects may be especially relevant for a variety of collisional plasmas such as plasma staircases [35], dense $Z$ pinches [36,37], and inertial confinement fusion implosions [38,39] where current-driven transport has a notable effect on hydrodynamic evolution and therefore yield.

*Data availability.* The data that support the findings of this article are openly available [40].

[1] A. R. Bell, R. G. Evans, and D. J. Nicholas, Elecron energy transport in steep temperature gradients in laser-produced plasmas, Phys. Rev. Lett. **46**, 243 (1981).

[2] J. D. Callen and M. W. Kissick, Evidence and concepts for non-local transport, Plasma Phys. Controlled Fusion **39**, B173 (1997).

[3] H. G. Rinderknecht, P. A. Amendt, S. C. Wilks, and G. Collins, Kinetic physics in ICF: Present understanding and future directions, Plasma Phys. Controlled Fusion **60**, 064001 (2018).
[4] D. Power, S. Mijin, M. Wigram, F. Militello, and R. Kingham, Scaling laws for electron kinetic effects in tokamak scrape-off layer plasmas, Nucl. Fusion **63**, 086013 (2023).
[5] G. Gregori, S. H. Glenzer, J. Knight, C. Niemann, D. Price, D. H. Froula, M. J. Edwards, R. P. J. Town, A. Brantov, W. Rozmus, and V. Y. Bychenkov, Effect of nonlocal transport on heat-wave propagation, Phys. Rev. Lett. **92**, 205006 (2004).
[6] Z. Chen, X. Yang, G. Zhang, Y. Ma, R. Yan, H. Xu, Z. Sheng, F. Shao, and J. Zhang, Role of nonlocal heat transport on the laser ablative Rayleigh-Taylor instability, Nucl. Fusion **64**, 126029 (2024).
[7] R. Y. Lau, D. J. Strozzi, M. Sherlock, M. Weis, A. S. Joglekar, W. A. Farmer, Y. Shi, and J. R. Cary, Nonlocal effects on thermal transport in MagLIF-relevant gaspipes on NIF, Phys. Plasmas **32**, 082104 (2025).
[8] N. B. Meezan, D. T. Woods, N. Izumi, H. Chen, H. A. Scott, M. B. Schneider, D. A. Liedahl, O. S. Jones, G. B. Zimmerman, J. D. Moody, O. L. Landen, and W. W. Hsing, Evidence of restricted heat transport in national ignition facility *Hohlraums*, Phys. Plasmas **27**, 102704 (2020).
[9] S. Chapman, T. G. Cowling, and D. Park, The mathematical theory of non-uniform gases, Am. J. Phys. **30**, 389 (1962).
[10] L. Spitzer, *Physics of Fully Ionized Gases*, 2nd ed. (Interscience, New York, 1962).
[11] S. I. Braginskii, *Reviews of Plasma Physics* (Consultants Bureau, New York, 1965), p. 205.
[12] E. M. Epperlein and M. G. Haines, Plasma transport coefficients in a magnetic field by direct numerical solution of the Fokker–Planck equation, Phys. Fluids **29**, 1029 (1986).
[13] J.-Y. Ji and E. D. Held, Closure and transport theory for high-collisionality electron-ion plasmas, Phys. Plasmas **20**, 042114 (2013).
[14] E. M. Epperlein and R. W. Short, A practical nonlocal model for electron heat transport in laser plasmas, Phys. Fluids B **3**, 3092 (1991).
[15] H. Zhao, Z. Sheng, and S. Weng, Nonlocal thermal transport in magnetized plasma along different directions, Matter Radiat. Extremes **7**, 045901 (2022).
[16] A. R. Bell and M. Sherlock, The fastvfp code for solution of the Vlasov–Fokker–Planck equation, Plasma Phys. Controlled Fusion **66**, 035014 (2024).
[17] A. Thomas, M. Tzoufras, A. Robinson, R. Kingham, C. Ridgers, M. Sherlock, and A. Bell, A review of Vlasov–Fokker–Planck numerical modeling of inertial confinement fusion plasma, J. Comput. Phys. **231**, 1051 (2012).
[18] G. P. Schurtz, P. D. Nicolaï, and M. Busquet, A nonlocal electron conduction model for multidimensional radiation hydrodynamics codes, Phys. Plasmas **7**, 4238 (2000).
[19] P. D. Nicolaï, J.-L. A. Feugeas, and G. P. Schurtz, A practical nonlocal model for heat transport in magnetized laser plasmas, Phys. Plasmas **13**, 032701 (2006).
[20] D. Del Sorbo, J.-L. Feugeas, P. Nicolaï, M. Olazabal-Loumé, B. Dubroca, S. Guisset, M. Touati, and V. Tikhonchuk, Reduced entropic model for studies of multidimensional nonlocal transport in high-energy-density plasmas, Phys. Plasmas **22**, 082706 (2015).
[21] J. P. Brodrick, R. J. Kingham, M. M. Marinak, M. V. Patel, A. V. Chankin, J. T. Omotani, M. V. Umansky, D. Del Sorbo, B. Dudson, J. T. Parker, G. D. Kerbel, M. Sherlock, and C. P. Ridgers, Testing nonlocal models of electron thermal conduction for magnetic and inertial confinement fusion applications, Phys. Plasmas **24**, 092309 (2017).
[22] C. Arran, M. Holec, M. Sherlock, M. Marinak, and C. P. Ridgers, The accuracy of multi-group models for nonlocal electron transport in magnetized plasmas, Phys. Plasmas **32**, 043908 (2025).
[23] J. R. Sanmartín, Electron heat conduction in ICF targets, in *Nuclear Fusion by Inertial Confinement*, edited by G. Velarde, Y. Ronen, and J. M. Martinez-Val (CRC Press, Boca Raton, FL, 1992), Chap. 7, pp. 185–196.
[24] M. Holec, J. Nikl, and S. Weber, Nonlocal transport hydrodynamic model for laser heated plasmas, Phys. Plasmas **25**, 032704 (2018).
[25] D. Bennaceur-Doumaz and A. Bendib, Nonlocal electron transport in magnetized plasmas with arbitrary atomic number, Phys. Plasmas **13**, 092308 (2006).
[26] H. C. Watkins, Studies of magnetised and non-local transport in laser-plasma interactions, Ph.D. thesis, Imperial College London, 2019.
[27] P. Helander and D. J. Sigmar, *Collisional Transport in Magnetized Plasmas* (Canbridge University Press, Cambridge, UK, 2002).
[28] N. T. Mitchell, D. A. Chapman, C. J. McDevitt, M. P. Read, and G. Kagan, A reduced kinetic method for investigating non-local ion heat transport in ideal multi-species plasmas, Plasma Phys. Controlled Fusion **66**, 075005 (2024).
[29] G. Kagan, D. Svyatskiy, H. G. Rinderknecht, M. J. Rosenberg, A. B. Zylstra, C.-K. Huang, and C. J. McDevitt, Self-similar structure and experimental signatures of suprathermal ion distribution in inertial confinement fusion implosions, Phys. Rev. Lett. **115**, 105002 (2015).
[30] M. Casanova, O. Larroche, and J.-P. Matte, Kinetic simulation of a collisional shock wave in a plasma, Phys. Rev. Lett. **67**, 2143 (1991).
[31] K. V. Lezhnin, S. R. Totorica, A. S. Hyder, J. Griff-McMahon, M. B. P. Adams, P. Tzeferacos, A. Diallo, and W. Fox, Particle-in-cell simulations of expanding high energy density plasmas with laser ray tracing, Phys. Plasmas **32**, 022701 (2025).
[32] W.-S. Zhang, H.-B. Cai, B. Du, D.-G. Kang, S.-Y. Zou, and S.-P. Zhu, Full particle-in-cell simulation of the formation and structure of a collisional plasma shock wave, Phys. Rev. E **103**, 023213 (2021).
[33] M. Luo, C. Heaton, Y. Wang, D. Plummer, M. Fitzgerald, F. Miniati, S. M. Vinko, and G. Gregori, Learning heat transport kernels using a nonlocal heat transport theory-informed neural network, Phys. Rev. Res. **7**, L042017 (2025).
[34] S. X. Hu, L. A. Collins, T. R. Boehly, J. D. Kress, V. N. Goncharov, and S. Skupsky, First-principles thermal conductivity of warm-dense deuterium plasmas for inertial confinement fusion applications, Phys. Rev. E **89**, 043105 (2014).
[35] N. Lopez, A. Bott, and A. Schekochihin, Collisional whistler instability and electron temperature staircase in inhomogeneous plasma, J. Plasma Phys. **91**, E45 (2025).

[36] J. P. Chittenden and M. G. Haines, Nernst and Ettinghausen effects in the dense $Z$-pinch: Their impact upon equilibria and runaway electrons, J. Phys. D: Appl. Phys. **26**, 1048 (1993).

[37] G. Farrow, J. P. Chittenden, and G. Kagan, Self-similar solutions for resistive diffusion, ohmic heating, and Ettingshausen effects in plasmas of arbitrary $\beta$, Phys. Plasmas **29**, 032703 (2022).

[38] C. Walsh, Extended magneto-hydrodynamic effects in indirect-drive inertial confinement fusion experiments, Ph.D. thesis, Imperial College London, 2018.

[39] C. A. Walsh, J. P. Chittenden, K. McGlinchey, N. P. L. Niasse, and B. D. Appelbe, Self-generated magnetic fields in the stagnation phase of indirect-drive implosions on the national ignition facility, Phys. Rev. Lett. **118**, 155001 (2017).

[40] https://github.com/Nic-Mitchell/CurrentDrivenTransport.